

PAPER • OPEN ACCESS

Spin structure of exclusive ω muoproduction at COMPASS

To cite this article: Bohdan Mariaski and on behalf of the COMPASS Collaboration 2020 *J. Phys.: Conf. Ser.* **1435** 012040

View the [article online](#) for updates and enhancements.



IOP | ebooksTM

Bringing you innovative digital publishing with leading voices to create your essential collection of books in STEM research.

Start exploring the collection - download the first chapter of every title for free.

Spin structure of exclusive ω muoproduction at COMPASS

Bohdan Mariański¹

(on behalf of the COMPASS Collaboration)

National Institute for Nuclear Research, PL 00-681 Warsaw, Poland

E-mail: b.marianski@ncbj.gov.pl

Abstract.

Spin Density Matrix Elements (SDMEs) are determined for exclusive ω meson production on unpolarized protons, in the COMPASS kinematic region of $1.0 \text{ (GeV/c)}^2 < Q^2 < 10.0 \text{ (GeV/c)}^2$, $5.0 \text{ GeV/c}^2 < W < 17.0 \text{ GeV/c}^2$ and $0.01 \text{ (GeV/c)}^2 < p_T^2 < 0.5 \text{ (GeV/c)}^2$. Using extracted the preliminary SDMEs values the hypothesis of S-Channel Helicity Conservation (SCHC) is studied. Certain matrix elements that correspond to the transition $\gamma_T^* \rightarrow V_L$ (e.g. r_{00}^5) indicate violation of SCHC in exclusive ω production. A sizable contribution of unnatural parity exchange amplitudes is found for exclusive ω meson muoproduction, and there is a clear indication of its decrease with increasing W . The extracted longitudinal-to-transverse cross section ratio is $0.553 \pm 0.044 \pm 0.020$.

1. Spin Density Matrix Elements

The study of Hard Exclusive Meson Production (HEMP) allows to constrain models of Generalized Parton Distributions (GPDs). If the produced particle is a vector meson we can get information on GPDs $GPDs H^{q(g)}(x, \xi, t)$, $E^{q(g)}(x, \xi, t)$, while exclusively produced pseudo-scalar mesons provide information on GPDs $\tilde{H}^{q(g)}(x, \xi, t)$, $\tilde{E}^{q(g)}(x, \xi, t)$. All these GPDs are called chiral-even because the helicity of struck parton is unchanged. When higher twist effects are included in the distribution amplitude, chiral odd or transversity $GPDs H_T^{q(g)}(x, \xi, t)$, $E_T^{q(g)}(x, \xi, t)$, $\tilde{H}_T^{q(g)}(x, \xi, t)$, $\tilde{E}_T^{q(g)}(x, \xi, t)$, $\bar{E}_T^{q(g)} = 2\tilde{H}_T^{q(g)} + E_T^{q(g)}$ with parton helicity flip can be constrained. These GPDs are not accessible in Deeply Virtual Compton Scattering (DVCS). Moreover, HEMP allows to study various quark-flavor combinations of GPDs and reaction mechanism. Most of this information we get from Spin Density Matrix Elements (SDMEs), which determine angular distributions of the particles from the decay of the vector meson. These elements are bilinear combinations of helicity amplitudes $F_{\lambda_V \lambda'_N \lambda_\gamma \lambda_N}$, where λ_γ is the virtual photon helicity and λ_V the vector-meson helicity, while λ_N and λ'_N are the helicities of the nucleon in the initial and final states, respectively.

In the $\gamma^* N$ Centre-of-Mass (CM) system the spin density matrix of the vector meson is given by the von Neumann equation [1]:

$$\rho_{\lambda_V \lambda'_V} = \frac{1}{2\mathcal{N}} \sum_{\lambda_\gamma \lambda'_\gamma \lambda_N \lambda'_N} F_{\lambda_V \lambda'_N \lambda_\gamma \lambda_N} \varrho_{\lambda_\gamma \lambda'_\gamma}^{U+L} F_{\lambda'_V \lambda'_N \lambda'_\gamma \lambda'_N}^* \quad (1)$$

¹ Work supported by the Polish NCN Grant 2017/26/M/ST2/00498



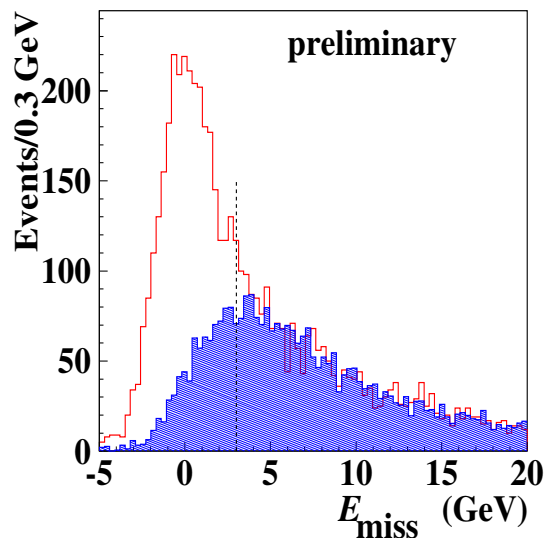


Figure 1. The E_{miss} distribution of data for exclusive ω production (red line) is compared with the SIDIS E_{miss} distribution from LEPTO MC (shaded blue area).

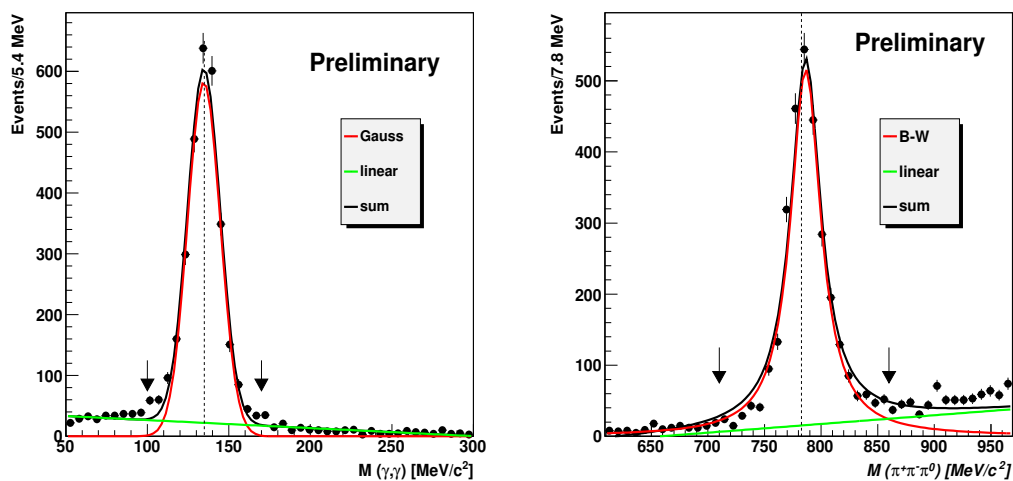


Figure 2. Left panel: Distributions of $\gamma\gamma$ invariant mass (left) fitted by Gaussian function and linear background. Dashed vertical line denotes PDG value. Right panel: Distributions of $\pi^+\pi^-\pi^0$ invariant mass (right) fitted by Breit-Wigner function and linear background. Vertical arrows denote cuts for the invariant mass. Dashed vertical line denotes PDG value.

LEPTO MC simulation reweighted in the same way as in Ref. [?]. The fraction of background for the entire kinematic region is 20 %. In Fig. 2 the distributions of the invariant mass of $\gamma\gamma$ and of $\pi^+\pi^-\pi^0$ are shown. After all cuts we have 3060 exclusive events.

3. Results for the entire kinematic region

The SDMEs for the entire kinematic region have been determined in the COMPASS kinematic region of $1.0 (\text{GeV}/c)^2 < Q^2 < 10.0 (\text{GeV}/c)^2$, $5.0 \text{ GeV}/c^2 < W < 17.0 \text{ GeV}/c^2$ and $0.01 (\text{GeV}/c)^2 < p_T^2 < 0.5 (\text{GeV}/c)^2$, which corresponds to $\langle Q^2 \rangle = 2.1 (\text{GeV}/c)^2$, $\langle W \rangle =$

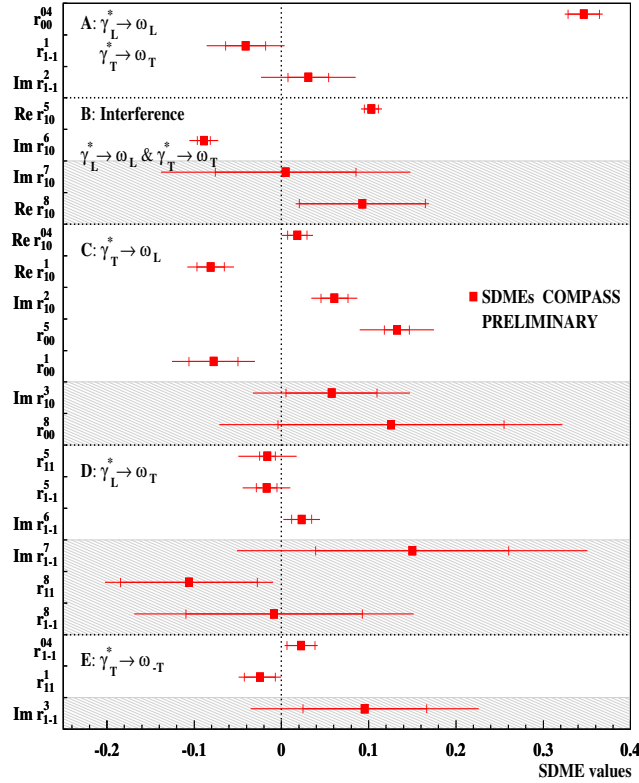


Figure 3. The 23 SDMEs extracted for exclusive ω production in the entire COMPASS kinematic region with $\langle Q^2 \rangle = 2.1$ (GeV/c) 2 , $\langle W \rangle = 7.6$ GeV/c 2 and $\langle p_T^2 \rangle = 0.16$ (GeV/c) 2 mean values. The inner error bars represent the statistical uncertainties, while the outer ones indicate the statistical and systematic uncertainties added in quadrature. SDMEs measured with unpolarized (polarized) beam are displayed in the unshaded (shaded) areas.

7.6 GeV/c 2 and $\langle p_T^2 \rangle = 0.16$ (GeV/c) 2 . Here, Q^2 represents the negative-square of the virtual-photon four-momentum, W the invariant mass of the photon-nucleon system and p_T^2 the squared transverse momentum of ω with respect to virtual photon γ^* . The preliminary SDMEs of the ω meson for the integrated data are presented in Fig. 3. The presented SDMEs are divided into five classes corresponding to different helicity transitions. Class A corresponds to the transition of longitudinal virtual photons to longitudinal mesons $\gamma_L^* \rightarrow V_L$ and transverse virtual photons to transverse mesons $\gamma_T^* \rightarrow V_T$. Class B corresponds to the interference of these two transitions. Class C corresponds to the $\gamma_T^* \rightarrow V_L$ transition, class D to the $\gamma_L^* \rightarrow V_T$ transition, and class E to the $\gamma_T^* \rightarrow V_{-T}$ transition.

In the case of SCHC only the seven SDMEs of class A and class B (r_{00}^{04} , r_{1-1}^1 , $\text{Im}\{r_{1-1}^2\}$, $\text{Re}\{r_{10}^5\}$, $\text{Im}\{r_{10}^6\}$, $\text{Im}\{r_{10}^7\}$, $\text{Re}\{r_{10}^8\}$), are not restricted to be zero, but six of them have to obey the following relations [1]: $r_{1-1}^1 = -\text{Im}\{r_{1-1}^2\}$, $\text{Re}\{r_{10}^5\} = -\text{Im}\{r_{10}^6\}$, $\text{Im}\{r_{10}^7\} = \text{Re}\{r_{10}^8\}$.

For these SDMEs we found: $r_{1-1}^1 + \text{Im}\{r_{1-1}^2\} = -0.01 \pm 0.038 \pm 0.047$, $\text{Re}\{r_{10}^5\} + \text{Im}\{r_{10}^6\} = 0.044 \pm 0.011 \pm 0.013$, $\text{Im}\{r_{10}^7\} - \text{Re}\{r_{10}^8\} = -0.088 \pm 0.110 \pm 0.196$.

These relations for classes A and B fulfill the requirements of SCHC. All other SDMEs are

required by SCHC to be zero. However, from Fig. 3 one can see that few SDMEs of class C, like $\text{Re } r_{00}^5$, $\text{Re } r_{10}^1$, $\text{Im } r_{10}^2$, are inconsistent with the hypothesis of SCHC. In the GK model [3] these SDMEs are related to transversity GPDs. The data presented here may help to constrain the model.

4. Contribution of UPE process in exclusive ω production

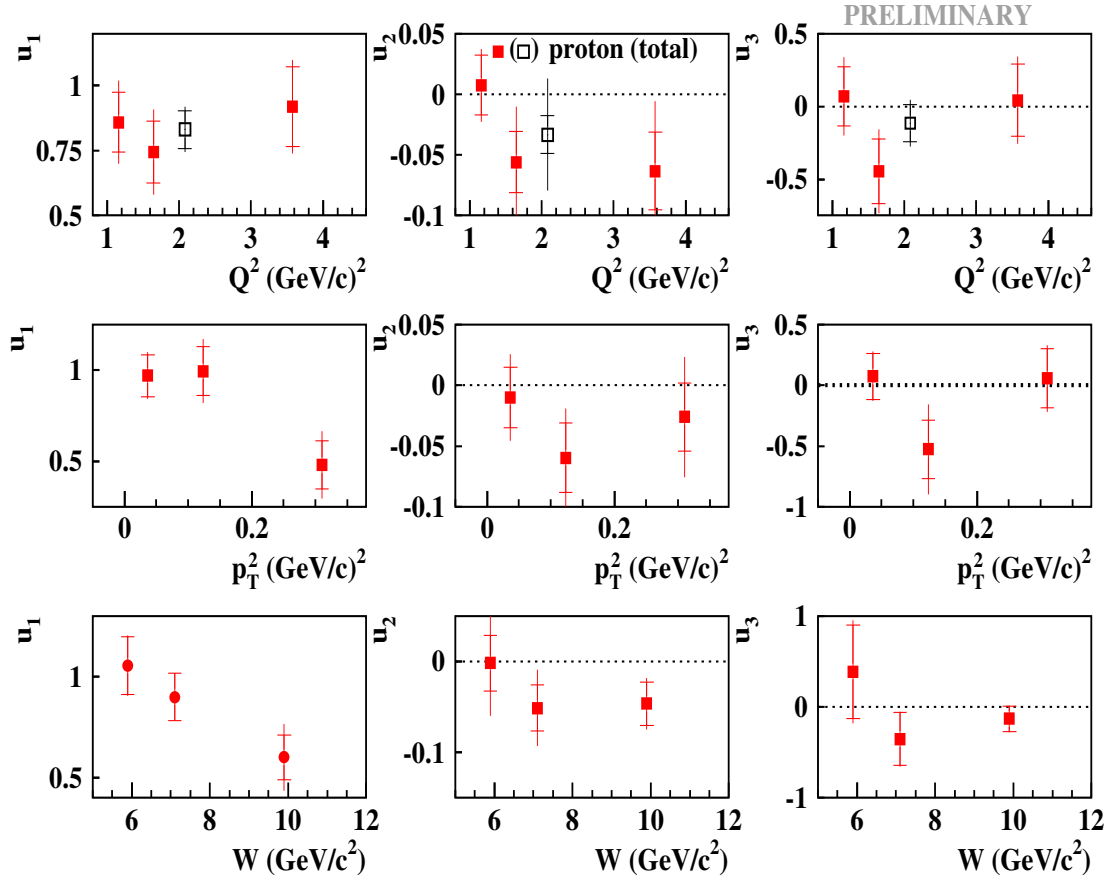


Figure 4. Q^2 , p_T^2 and W dependences of u_1 , u_2 , u_3 . The open symbols represent the values over entire kinematic region. The inner error bars represent the statistical uncertainties, while the outer ones indicate the statistical and systematic uncertainties added in quadrature.

The existence of UPE contribution in exclusive ω production can be tested by examining linear combination of SDMEs such as

$$u_1 = 1 - r_{00}^{04} + 2r_{1-1}^{04} - 2r_{11}^1 - 2r_{1-1}^1. \quad (3)$$

The quantity u_1 can be expressed in terms of helicity amplitudes as

$$u_1 = \frac{\sum 4\epsilon |U_{10}|^2 + 2|U_{11} + U_{-11}|^2}{\mathcal{N}}. \quad (4)$$

As one can see the numerator depends only on UPE amplitudes. Therefore a u_1 with value different from zero would indicate a contribution of UPE processes. For the entire kinematic

region of COMPASS u_1 is equal to $0.830 \pm 0.073 \pm 0.049$, which is a signal of large UPE contribution. An additional information one gets from the following combinations

$$u_2 = r_{11}^5 + r_{1-1}^5, \quad (5)$$

$$u_3 = r_{11}^8 + r_{1-1}^8. \quad (6)$$

When expressed in terms of helicity amplitudes, the quantities u_2 and u_3 combine to

$$u_2 + iu_3 = \sqrt{2} \sum \widetilde{\frac{(U_{11} + U_{-11})U_{10}^*}{\mathcal{N}}}. \quad (7)$$

For COMPASS we get $u_2 = -0.033 \pm 0.016 \pm 0.043$ and $u_3 = -0.114 \pm 0.126 \pm 0.099$

In Fig. 4 the dependence of quantities u_1 , u_2 , u_3 on Q^2 , p_T^2 and W is presented. As one can see u_1 decreases with increasing W and p_T^2 , which indicate that UPE contributions becomes smaller, while u_2 , u_3 fluctuate around zero.

5. Longitudinal-to-transverse cross section ratio

Usually, the longitudinal-to-transverse virtual-photon differential cross section ratio

$$R = \frac{d\sigma_L(\gamma_L^* \rightarrow V)}{d\sigma_T(\gamma_T^* \rightarrow V)}$$

is experimentally determined using the measured SDME r_{00}^{04} and the approximate relation [4].

$$R \approx \frac{1}{\epsilon} \frac{r_{00}^{04}}{1 - r_{00}^{04}}. \quad (8)$$

This relation is exact in the case of SCHC. The obtained ratio R is equal to $0.553 \pm 0.044 \pm 0.020$. The kinematic dependences of the longitudinal to transverse virtual-photon differential cross-section ratio are shown in Fig. 5. It is seen that the ratio increases as Q^2 and p_T^2 increase.

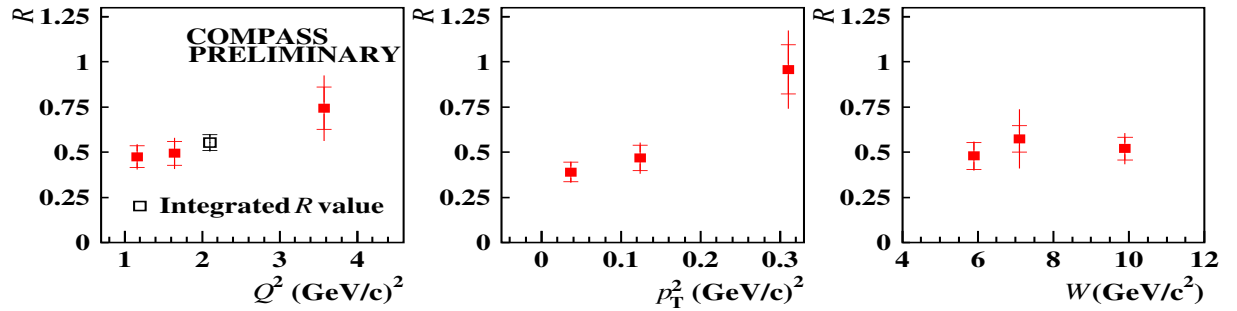


Figure 5. Q^2 , p_T^2 and W dependences of the longitudinal-to-transverse cross section ratio R . The open symbol represents the value over entire kinematic region. The inner error bars represent the statistical uncertainties, while the outer ones indicate the statistical and systematic uncertainties added in quadrature.

References

- [1] K Schilling K and Wolf G 1973 How to analyze vector mesonproduction in inelastic scattering *Nucl. Phys. C* **61** 361
- [2] HERMES Collaboration 2009 Spin Density Matrix Elements in Exclusive ρ^0 Electroproduction on ^1H and ^2H Targets at 27.5 GeV Beam Energy *Eur.Phys. J. C* **62** 659
- [3] Goloskokov S and Kroll P 2009 The target asymmetry in hard vector-meson electroproduction and parton angular momenta *Eur. Phys. J. C* **59** 809
- [4] HERMES Collaboration 2014 Spin Density Matrix Elements in Exclusive ω Electroproduction on ^1H and ^2H Targets at 27.6 GeV Beam Energy *Eur. Phys. J. C* **74** 3110 Erratum: 2016 *Eur. Phys.J. C* **76** 162